

Embedding nuclear physics inside the unitary window

M. Gattobigio,¹ A. Kievsky,² and M. Viviani²

¹*Université Côte d'Azur, CNRS, Institut de Physique de Nice,
1361 route des Lucioles, 06560 Valbonne, France*

²*Istituto Nazionale di Fisica Nucleare, Largo Pontecorvo 3, 56100 Pisa, Italy*

The large values of the singlet and triplet scattering lengths locate the two-nucleon system close to the unitary limit, the limit in which these two values diverge. As a consequence, the system shows a continuous scale invariance which strongly constrains the values of the observables, a well-known fact already noticed a long time ago. The three-nucleon system shows a discrete scale invariance that can be observed by correlations of the triton binding energy with other observables as the doublet nucleon-deuteron scattering length or the alpha-particle binding energy. The low-energy dynamics of these systems is universal; it does not depend on the details of the particular way in which the nucleons interact. Instead, it depends on a few control parameters, the large values of the scattering lengths and the triton binding energy. Using a potential model with variable strength set to give values to the control parameters, we study the spectrum of $A = 2, 3, 4, 6$ nuclei in the region between the unitary limit and their physical values. In particular, we analyze how the binding energies emerge from the unitary limit forming the observed levels.

I. INTRODUCTION

In a non-relativistic theory where one allows for a tunable potential (or other parameters like the mass m of the particles), we refer to the unitary window as to the range of those parameters for which the scattering(s) length(s) a attains a value close to infinity (the unitary limit). This is a relevant limit because the physics becomes universal [1] and a common description can be used for totally different systems, ranging from nuclear physics up to atomic physics or down in scale to hadronic systems. For instance, in the two-body sector there is the appearance of a shallow (real or virtual) bound state whose energy is governed by the scattering length, $E_2 = -\hbar^2/ma^2$. This state is shallow if compared with the energy related to the typical interaction length ℓ , defined as $-\hbar^2/m\ell^2$, and in the limit $a/\ell \rightarrow \infty$, where it becomes resonant. This limit can be understood either as the scattering length going to infinity or as the range of the interaction going to zero; in the last case one talks of zero-range limit or scaling limit.

In the scaling limit, the two-body sector displays continuous scale invariance due to the fact that the only dimensionful parameter is the scattering length. As soon as we change the number of particles, the above symmetry is dynamically broken to a discrete scale invariance (DSI); for example, for three equal bosons at the unitary limit, an infinite tower of bound states appears - the Efimov effect [2, 3] - related by a discrete scale transformation $r \rightarrow \exp(\pi/s_0)r \approx 22.7r$, with the scaling factor $s_0 = 1.0062\dots$ a universal transcendental number that does not depend on the actual physical system. The anomalous breaking of the symmetry gives rise to an emergent scale at the three-body level which is usually referred to as the three-body parameter κ_* , giving the binding energy $\hbar^2\kappa_*^2/m$ of a reference state of the above tower of states.

The fine tuning of the parameters that brings a systems inside the unitary window can be realized either

artificially, like it has been the case in the field of cold atoms with Feshbach resonances [4], or can be provided by nature, as in the case of atomic ^4He , where the $^4\text{He}_2$ molecule has a binding energy of several order smaller than the typical interaction energy [5]. Nuclear physics is another example of tuned-by-nature system; the binding energy of the deuteron, $B_d = 2.22456$ MeV is much smaller than the typical-nuclear energy $\hbar^2/m\ell^2 \approx 20$ MeV, considering that the interaction length is given by the inverse of the pion mass m_π , $\ell \sim 1/m_\pi \approx 1.4$ fm. The fact that nuclear physics resides inside such a window has been used in the pioneering works of the thirties where the binding energies of light nuclei have been calculated using either boundary conditions [6, 7] or pseudopotentials [8].

Nuclear physics is the low energy aspect of the strong interaction, namely Quantum Chromo Dynamics (QCD); in this limit, QCD is a strong interacting quantum field theory and only non-perturbative approaches could be used to describe the spectrum of nuclear physics. Such non-perturbative approaches start to appear, one example being Lattice QCD (LQCD); however, a complete calculation of nuclear properties seems at present not yet feasible using these techniques. Historically, the description of light nuclear systems were based on potential models constructed to reproduce a selected number of observables; first attempts have been based on the expansion of the potential on the most general operator basis compatible with the symmetries observed in the spectrum. Lately, it has been realized that a potential could be constructed starting from the symmetries of QCD in an Effective Field Theory (EFT) approach. One of the important symmetry of QCD in the limit of zero-mass light quarks is the Chiral Symmetry; this symmetry is indeed spontaneous broken and its Goldstone boson is the π -meson. The mass of the pion m_π is not really zero because of the soft breaking term introduced by the explicit mass of the quarks up and down, but still is much lower than the typical hadronic masses. The chi-

ral limit is not the only interesting limit in QCD; the actual mass of the pion is probably close to a value for which the nucleon-nucleon scattering lengths diverge [9]; in fact, one can study the variation of the 1S_0 (singlet) a_0 and 3S_1 (triplet) a_1 scattering lengths as a function of the masses of the up and down quarks, or equivalently of m_π which is related to the quark mass by the Gell-Mann-Oakes-Renner relation. It has been shown that for $m_\pi \approx 200$ MeV both scattering lengths go to infinity [10, 11]. At the physical point, $m_\pi \approx 138$ MeV, the values of the two scattering lengths, $a_0 \approx -23.7$ fm and $a_1 \approx 5.4$ fm, are still (much) larger than the typical interaction length $\ell \approx 1.4$ fm; this is a further indication that nuclear physics is close to the unitary limit and well inside the universal window.

A model-independent description of the physics inside the unitary window is given by an EFT based on the clear separation of scales between the typical momenta $Q \sim 1/a$ of the system and the underlying high momentum scale $\sim 1/\ell$ [12–14]. Using EFT, if the power-counting is correct [15], one can systematically improve the prediction on observables. For instance, in the two-body sector the usual effective range expansion (ERE) can be reproduced by such an expansion [12]; the leading order (LO), which is just a two-body contact interaction, captures all the information encoded in the scattering length a , while the next-to-the-leading order term (NLO), which contains derivatives, captures the information encoded in the effective range r_e . Starting from the three-body sector, a LO three-body interaction is necessary [13, 14, 16] which introduces the emergent three-body scale.

It is possible to investigate the universal window by using potential models; this approach allows to follow the behaviour of two- and three-particle binding energies inside the window of universality. Also a higher number of particles can be considered as in Refs. [17–19] where it has been shown that the use of a simple Gaussian potential gives a good description of bosonic systems like Helium droplets in this regime.

In this paper we want to explore the window of universality for nucleons, that means for fermions with 1/2 spin and isospin degrees of freedom; the idea is to follow, as a function of the interaction range, the states which represent light nuclei in the region of universality and to observe which part of the nuclear spectrum is in fact governed by universality. The major difference with respect the bosonic case is the presence of two scattering lengths. There has been previous studies of the Efimov physics with two scattering lengths [11, 20–25], and there are different ways to explore the space of parameters; one possible choice is to keep constant the ration between the scattering lengths a_0/a_1 , selecting some cuts for in that space. Accordingly, we explore the nuclear cut, that means $a_0/a_1 \approx -4.3$, moving from the unitary point, $a_0, a_1 \rightarrow \infty$, to the physical point; at a more fundamental level, this is equivalent to change the mass of the pion m_π (or the sum of up and quark masses in QCD), as it

was shown in Refs. [10, 26]. Interestingly, we observe that, at unitary, in addition to the $A = 5$ gap we observe a $A = 6$ gap.

The paper is organized as follows. In Section II we will show how the spectrum of $A = 2, 3, 4, 6$ nucleons representing light nuclei depend on the scattering lengths when we change them from the unitary limit to the their real value, and we discuss what are the aspects of the universality of Efimov physics that still remain. In Section III we concentrate our study at the physical point, where a three-body force, as well as the Coulomb interaction, are introduced. In Section IV we investigate the possible rôle of p -waves in the binding of $A = 6$ nuclei. Finally, in Section V we give our conclusions.

II. 1/2 SPIN-ISOSPIN ENERGY LEVELS CLOSE TO UNITARY

In this section, we describe the discrete spectrum of spin 1/2- isospin 1/2 particles from the unitary limit to the point where nuclear physics is located, the physical point, defined as the point in which the scattering lengths take their observed values. To this end we construct the Efimov plot, a plot in the plane $(K, 1/a)$ defined by the energy momentum K of the bound state with energy $\hbar^2 K^2/m$, as a function of the inverse of the two-body scattering length a . In the case of two nucleons there are two different scattering lengths, a_0 and a_1 , in spin-isospin channels with $S, T = 0, 1$ and $S, T = 1, 0$ respectively. Accordingly, following Refs. [21, 22], the plane is defined with the triplet scattering length $(K, 1/a_1)$, taking care that for each value of a_1 , a_0 is varied accordingly maintaining the ratio a_0/a_1 constant. In Refs. [21, 22], the main characteristic of the Efimov plot for three 1/2 spin-isospin particles have been studied. In particular it was shown that for the ratio $a_0/a_1 \approx -4.3$, corresponding to the nuclear physics case, the infinite tower of states at unitary disappear very fast as a_1 decreases and, at $a_1 < 20$ fm, only one state survives. This simple analysis explains the existence of only one bound state for ^3H and ^3He . Conversely, in the case of three identical bosons, calculations using finite-range potentials have shown that the first excited state survive along the unitary window.

A. The potential model

In order to explore the unitary window through the Efimov plot, we calculate the binding energies of A nucleons for different values of the two-body scattering lengths. In the case of a zero-range interaction the $A = 2$ energy of the real (virtual) state for $a > 0$ ($a < 0$) is simply $E_2 = -\hbar^2/ma^2$. For three particles, and using a zero-range interaction, the binding energies can be obtained by solving the Faddeev zero-range equations encoded in the Skorniakov-Tern-Martirosian equations (see

Ref. [1] and references there in for details). It is well known that the contact interaction can be represented by different functional forms introducing finite-range effects. In particular, as it has been shown in Ref. [27], inside the unitary window a Gaussian potential captures the main characteristics of the dynamics, confirming the universal behavior of the system in this particular region. Considering that, for two nucleons, there are four different spin-isospin channels with quantum numbers $ST = 01, 10, 00, 11$, we define the following spin-isospin dependent potential of a Gaussian type

$$V(r) = \sum_{ST} V_{ST} e^{-(r/r_{ST})^2} \mathcal{P}_{ST}, \quad (1)$$

where we have introduced the spin-isospin \mathcal{P}_{ST} projectors. The minimal requirement to construct a fully antisymmetric two-body wave function with the lowest value of the angular momentum L is to consider the spin-isospin channels $S = 0, T = 1$ and $S = 1, T = 0$. Therefore, in this first analysis, the other two components of the potential are set to zero: $V_{00} = V_{11} = 0$. In each of the two remaining terms there are two parameters, the strength of the Gaussian and its range; we fix both ranges to be the same $r_{10} = r_{01} = r_0 = 1.65$ fm, and of the order of the nuclear range. With this choice an acceptable description of the two-body low-energy data is obtained (a refinement of the model will be discussed in the next section). The tuning of the two strengths allows us to control the scattering lengths; the value of V_{01} defines the singlet scattering length a_0 , while the value of V_{10} defines triplet one a_1 . In all our calculations we fix the value of the nucleon mass m so that $\hbar^2/m = 41.47$ MeV fm². In some of the following Table/Figures, as unit length we use we use $r_0 = 1.65$ fm and as unit of energy we use $E_0 = \hbar^2/mr_0^2 = 15.232$ MeV.

In order to calculate the binding energies for the nuclear systems having $A = 3, 4, 6$, we have solved the Schrödinger equation using two different variational methods. One method is based on the Hyperspherical Harmonic (HH) [28] basis in its unsymmetrized version [29–31]. We have used this approach mainly for $A = 3, 4$ since it is very accurate for states far from thresholds. Close to a threshold, as for $A = 6$ or for excited states in $A = 3, 4$, the dimension of the basis tends to become too big to have a good precision. To overcome this problem we implemented a version of the stochastic variational method (SVM) [32] with correlated-Gaussian functions as basis set; this method allows for a more economical description of the excited states close to the threshold.

By giving values to V_{10} and V_{01} , the values of the scattering lengths vary along the nuclear cut defined from the ratio $a_0/a_1 = -4.3066$. Along this path we have calculated the binding energies of $A = 2, 3, 4, 6$ nucleon systems. The calculations, for selected values of the potential strengths, are reported in Table I in the case of positive triplet-scattering length values, for which a two-body bound state in the 3S_1 channel exists. The cal-

culations cover a region between the unitary point, for which both scattering lengths attain an infinite value, and the physical point, for which the value of the two-body state is $E_2 = -2.2255$ MeV (the experimental binding energy of the deuteron is 2.224575(9) MeV), and the two scattering lengths have the values $a_1 = 5.4802$ fm and $a_0 = -23.601$ fm, with the experimental values $a_1 = 5.424(3)$ fm and $a_0 = -23.74(2)$ fm, respectively.

Considering the potential of Eq.(1) in all cases the lowest state corresponds to total orbital angular momentum $L = 0$. Moreover, in this first analysis the Coulomb interaction between protons were disregarded, so the isospin is conserved. In the three-body sector, the quantum numbers of ${}^3\text{H}$ and of ${}^3\text{He}$ are $S = 1/2$ and $T = 1/2$. In this exploration we disregarded other charge-symmetry breaking terms, accordingly the two nuclei have the same energy. We refer to their ground-state energy as E_3 and to their excited-state energy as E_3^* . The total wave function is antisymmetric with the spatial wave function mostly symmetric. We would like to stress a big difference between the bosonic and the nuclear cut already mentioned above: in the bosonic case the first excited state never disappears into the particle-dimer continuum whereas, in the nuclear case, the excited state disappear in the continuum and it becomes a virtual state already at a large value of a_1 ($a_1 \approx 20$ fm). The motivation is the following: at unitary, since we are using the same range for both gaussians, the system is equivalent to a bosonic system and an infinite set of excited states appears showing the Efimov effect (in Table I only the first one is reported). Moreover, the system is completely symmetric, no other symmetry is present. As the strength of the potentials starts to vary, keeping the ratio a_0/a_1 constant, the three-body wave function develops a spatial mixed symmetry component making the energy gain slower than in the bosonic case. The two-body system is not affected by the singlet potential (which is smaller) and its energy gain is the same as in the bosonic case; as a consequence the first excited state crosses the particle-dimer continuum becoming a virtual state.

From the results reported in Table I we also observe that the three-body binding energy at the physical point is much larger than the experimental value of -8.48 MeV; this is a well known fact related to the necessity of including a three-body force, a point we discuss in the next section. In Fig. 1 we show the Efimov plot up to four particles; we clearly see the three-body excited state disappearing in the continuum. We also observe the usual feature of two four-body states attached to the three-body ground state. The four body calculations are done for the same quantum numbers as ${}^4\text{He}$, that means $S = 0$ and $T = 0$, thus the two states have mostly a symmetric spatial wave function. The ratio between the ground state energy of the four-body state and the ground state of the three-body state E_4/E_3 is not constant along the path, but it varies from $E_4/E_3 = 5.89$ at the unitary point to $E_4/E_3 = 3.89$ at the physical point, close to the realistic case of 3.67. As far as the excited stated of

TABLE I. Calculations belonging to the nuclear cut, $a_0/a_1 = -4.3066$ for selected values of the strengths V_{01} and V_{10} . The ground-state energy E_A and, if it exists, the excited-state energy E_A^* of the A -particle system are reported. In the $A = 6$ case we distinguish between the total isospin $T = 1$ and total spin $S = 0$ case, ${}^6\text{He}$, and the $T = 0, S = 1$ case, ${}^6\text{Li}$. The Coulomb interaction is not taken into account.

$V_{10}(\text{MeV})$	$V_{01}(\text{MeV})$	$a_1(\text{fm})$	$E_2(\text{MeV})$	$E_3(\text{MeV})$	$E_3^*(\text{MeV})$	$E_4(\text{MeV})$	$E_4^*(\text{MeV})$	${}^6\text{He}(\text{MeV})$	${}^6\text{Li}(\text{MeV})$
-60.575	-37.9	5.4802	-2.2255	-10.2455	-	-39.843	-11.19	-41.60	-46.74
-60.	-37.95858685	5.5980	-2.1098	-10.0056	-	-39.221	-10.93	-40.87	-45.82
-58.	-38.17113668	6.0683	-1.72703	-9.19027	-	-37.093	-10.01	-38.36	-42.71
-56.	-38.39860618	6.6607	-1.37621	-8.40544	-	-35.017	-9.14	-35.95	-39.67
-54.	-38.64295075	7.4310	-1.05929	-7.65258	-	-32.997	-8.31	-33.58	-36.77
-52.	-38.90658498	8.4756	-0.77842	-6.93330	-	-31.035	-7.52	-31.31	-33.95
-50.0	-39.19224	9.97497	-0.53599	-6.24929	-	-29.135	-6.78	-	-31.23
-48.0	-39.50320907	12.31255	-0.334659	-5.60235	-	-27.300	-6.08	-	-28.62
-46.0	-39.8434712	16.47151	-0.17735880	-4.99446	-	-25.536	-5.43	-	-26.17
-45.0	-40.026055	20.06376	-0.1163	-4.7058	-0.116853	-24.682	-5.13	-	-24.96
-44.5	-40.120751	22.6040702	-0.0903760	-4.5654	-0.091991	-24.262	-4.98	-	-24.41
-44.0	-40.217947	25.95893	-0.067559	-4.4278	-0.07054	-23.847	-4.83	-	-
-43.5	-40.3174375	30.5953	-0.047939	-4.2927	-0.053034	-23.437	-4.69	-	-
-43.0	-40.4196253	37.421571	-0.0315796	-4.1605	-0.03853	-23.032	-4.55	-	-
-42.5	-40.52452499	48.46985	-0.0185467	-4.0311	-0.02697	-22.633	-4.42	-	-
-42.0	-40.63225234	69.413066	-0.0089083	-3.9044	-0.01816	-22.238	-4.28	-	-
-41.5	-40.74293099	124.3314	-0.00273453	-3.7807	-0.01186	-21.850	-4.15	-	-
-40.88363	-40.88363	∞	0	-3.6322	-0.00678	-21.378	-4.00	-	-

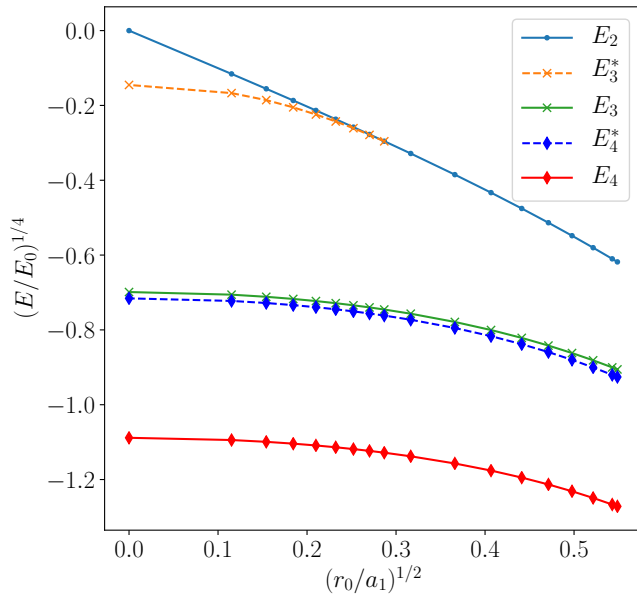


FIG. 1. Efimov plot for $N = 2, 3, 4$ particles along the nuclear cut $a_0/a_1 = -4.3066$. The triplet scattering length a_1 is in units of $r_0 = 1.65$ fm and the energies are expressed in units of $E_0 = \hbar^2/mr_0^2 = -15.232$ MeV.

the four-body system is concerned, the ratio between its energy and that of the three-body state is more or less constant along the path $E_4^*/E_3 = 1.09 - 1.1$; the finite-

range corrections result in a bigger value of this ratio with respect to the zero-range limit [33].

B. Universal behavior

To analyse the universal behavior of the few-nucleon systems we start recalling the Efimov radial law for three equal bosons [1]

$$E_3/E_2 = \tan^2 \xi \quad (2a)$$

$$\kappa_* a = e^{(n-n_*)\pi/s_0} \frac{e^{-\Delta(\xi)/2s_0}}{\cos \xi}, \quad (2b)$$

where, due to its zero-range character, $E_2 = -\hbar^2/ma^2$ and the three-body binding energy of level n_* at unitary is $\hbar^2/m\kappa_*^2$. The function $\Delta(\xi)$ is universal in the sense that it is the same for all the energy levels. It can be calculated solving the STM equations as explained for example in Ref. [1], and its expression can be given in a parametric form [34]. To be noticed that the spectrum given by the above equation is not bounded from below. For a real three-boson system located close to the unitary limit and interacting through short-range forces with a typical length ℓ , the discrete spectrum is bounded from below with the number of levels roughly approximate by $(s_0/\pi) \ln(|a|/\ell)$.

The extension of Eqs. (2) to describe finite-range interactions, considering more particles and eventually spin-isospin degrees of freedom, is given in a series of papers,

Refs.[18, 21, 22, 35, 36], and it reads

$$E_A^m/E_2 = \tan^2 \xi \quad (3a)$$

$$\kappa_A^m a_B + \Gamma_A^m = \frac{e^{-\Delta(\xi)/2s_0}}{\cos \xi}, \quad (3b)$$

where for three particles, E_3^m , $m = 0, 1, \dots$, is the energy of the different branches; in Fig. 1 the first two branches ($m = 0, 1$) are shown. For four particles E_4^m , $m = 0, 1$, is the energy of the two states attached to the lowest three-body branch, E_3^0 . The length a_B is defined from the two-body energy as $E_2 = -\hbar^2/ma_B^2$. Finally, we have introduced the shift parameter, Γ_A^m , which results almost constant along the unitary window. A recent analysis of the shift parameter for three equal bosons is given in Ref. [34], where it is related to the running three-body parameter introduced in Ref. [37]. Eq. (3b) can also be written as

$$\kappa_A^m a_B = \frac{e^{-\Delta_A^m(\xi)/2s_0}}{\cos \xi}, \quad (4)$$

where the shift Γ_A^m is absorbed in the level function $\Delta_A^m(\xi)$; in the present work it is calculated from a Gaussian potential as in the Bosonic case [27]. In Ref. [27] it has been shown that the level function $\Delta_A^m(\xi)$, which incorporates the finite-range corrections given by a Gaussian potential, is about the same for different potentials close to the unitary limit. Accordingly a Gaussian potential can be thought as a universal representation of potential models inside the universality window. Moreover, the level function $\Delta_A^m(\xi)$ is unique for all Gaussian potentials, it does not depend on the particular range r_0 used for the actual calculations because, as shown in Fig. 1, this parameter is just used to have a dimensionless scattering length and energy. This is an important point because the limit $r_0/a_1 \rightarrow 0$ can be read either as $a_1 \rightarrow \infty$ or as $r_0 \rightarrow 0$. In the limit $r_0/a_1 = 0$ the unitary point coincides with the finite-range-regularized scaling-limit point and the dimensionless values of the binding momenta are the same for all Gaussian potentials. They are given in Tab. II for $A = 3, 4$ and $m = 0, 1$.

The uniqueness of the Gaussian-level functions and the fact that the Gaussian potential is an universal representation of potential models close to the unitary limit, allows us to use the Gaussian potential to predict the values of the energies at the unitary limit for real systems, which in principle are described by more realistic potentials. We proceed in the following way: from Eq. (2) we observe that the product $\kappa_* a$ is a function of the only angle ξ through the universal function $\Delta(\xi)$. This property is related to the DSI and it is well verified for real systems, which, close to the unitary limit, are well represented by the Gaussian level functions as given in Eq. (4). Therefore, the product $\kappa_A^m a_B$ is function of solely the angle ξ verifying the following equality

$$\kappa_A^m a_B \Big|_{\text{exp}} = \kappa_A^m a_B \Big|_G, \quad (5)$$

TABLE II. In this table we report the universal-Gaussian values of the momentum energies of $A = 3, 4$ systems at the unitary point for the branches $m = (0, 1)$, and we summarise the values of the physical angles, of the Gaussian two-body binding energies corresponding to the same angle reproduced by the Gaussian potential, and of the momentum and energy at the unitary limit for the real-nuclear systems that we have predicted using Eq. (6).

A	m	$r_0 \kappa_A^m \Big _G$	$\tan^2 \xi \Big _{\text{exp}}$	$a_B/r_0 \Big _G$	$\kappa_A^m \Big _{\text{exp}} \text{ (fm}^{-1}\text{)}$	$E_A^m \Big _{\text{exp}} \text{ (MeV)}$
3	0	0.4883	3.81	2.1866	0.2473	2.536
3	1	0.0211				
4	0	1.1847	13.13	2.0774	0.570	13.474
4	1	0.5124				

where $\kappa_A^m a_B \Big|_{\text{exp}}$ is the function evaluated at the angle given by the experimental values, and the function $\kappa_A^m a_B \Big|_G$ is evaluated at the same angle but calculated with the gaussian potential. From Eq. (5) the energy momentum at unitary for the real systems is

$$\kappa_A^m \Big|_{\text{exp}} = \frac{1}{a_B} \Big|_{\text{exp}} \kappa_A^m a_B \Big|_G = \frac{1}{a_B} \Big|_{\text{exp}} (r_0 \kappa_A^m) \frac{a_B}{r_0} \Big|_G, \quad (6)$$

where the universal Gaussian values of $r_0 \kappa_A^m \Big|_G$ are reported in Table II.

We can apply Eq. (6) to predict the value of the three- and four-body energies at the unitary limit for nuclear physics. For the three-body case, the experimental binding energies of the deuteron, $a_B \Big|_{\text{exp}} = 4.3176$ fm, and of the ^3H fix the experimental value of the angle ξ to be $\tan^2 \xi \Big|_{\text{exp}} = 3.81$. Using the range value $r_0 = 1.65$ fm, this angle is reproduced by the Gaussian strengths $V_{10} = -64.96$ MeV and $V_{01} = -37.4855$ MeV, which corresponds to a deuteron energy of $E_2 = -3.1858639$ MeV, or, equivalently, $a_B/r_0 \Big|_G = 2.1866$. Using the Gaussian value of $r_0 \kappa_3^0 \Big|_G = 0.4883$, from Eq. (6) we obtain $\kappa_3^0 \Big|_{\text{exp}} = 0.2473$ fm $^{-1}$ corresponding to a three-nucleon binding energy at unitary of $E_3^0 \Big|_{\text{exp}} = 2.536$ MeV.

We proceed in the same way for the four-body case. We take $E_4^0 = 29.1$ MeV as the experimental value of ^4He without Coulomb interaction [38]; with this value and that of the deuteron we obtain $\tan^2 \xi \Big|_{\text{exp}} = 13.1$, which can be reproduced using the Gaussian potential with $V_{10} = -66.4$ MeV and $V_{01} = -37.36047$ MeV that also gives $a_B/r_0 \Big|_G = 2.0774$. Using Eq. (6) and the universal-Gaussian value $r_0 \kappa_4^0 \Big|_G = 1.1847$ we obtain $\kappa_4^0 \Big|_{\text{exp}} = 0.570$ fm $^{-1}$, or, equivalently, $E_4^0 \Big|_{\text{exp}} = 13.474$ MeV. All the results are summarised in Table II, and it should be noted that predictions of the same order exist for $A = 3$ [10].

In order to study further the close relation between the zero- and finite-range descriptions we look at the behavior of

$$y(\xi) = e^{-\Delta(\xi)/2s_0} / \cos \xi \quad (7)$$

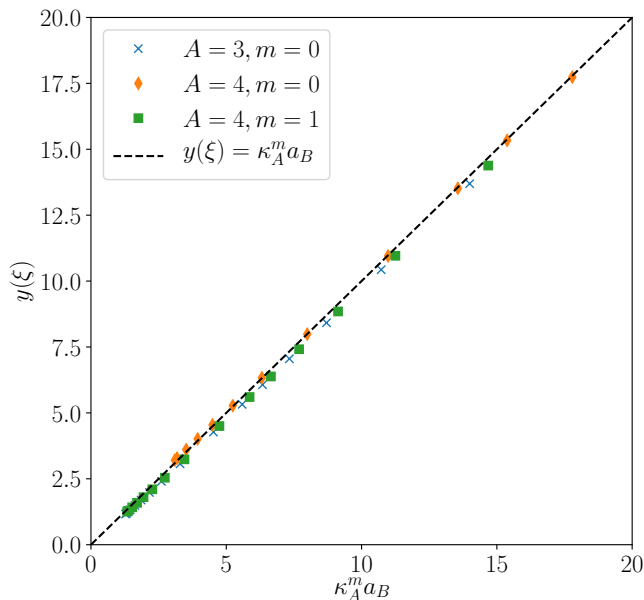


FIG. 2. Efimov plot for the nuclear cut in the form of $y(\xi)$, Eq. (7), as a function of $\kappa_A^m a_B$. The zero-range limit is given by the straight line $y(\xi) = \kappa_A^m a_B$.

as a function of $\kappa_A^m a_B$. For zero-range this function is a line going through the origin at 45 degrees. As already observed [27, 35] for bosons, if the shift parameter Γ_A^m is almost constant, three and four particles results should give a linear relation between $y(\xi)$ and $\kappa_A^m a_B$ though not going through the origin. The results are given in Fig. 2 showing the expected behavior in a very extended range of $\kappa_A^m a_B$ values.

C. Including the $A = 6$ energies

In the following we study the six-body bound states as a function of the triplet scattering length along the nuclear cut; we expect a bigger deviation from the bosonic case because the totally symmetric spatial component cannot be anymore present; with only four internal degrees of freedom, the spin and the isospin, there are only mixed components. In the $A = 6$ case we distinguish two different states, one with quantum numbers $S = 0$ and $T = 1$, to which we refer to as ${}^6\text{He}$ even in absence of Coulomb interaction, and one with quantum numbers $S = 1$ and $T = 0$, to which we refer to as ${}^6\text{Li}$. The results of Table I are reported in Fig. 3; clearly, we can observe the absence of these states close to the unitary limit. This is a big difference with respect to the bosonic case, where, for $6 \geq A > 3$ the A -boson system at unitary has two states, one deep and one shallow, attached to the $A - 1$ ground state [18, 35, 39]. Instead, the two fermionic $A = 6$ states are not bound below the ${}^4\text{He}$ threshold (at unitary the ${}^4\text{He}$ and ${}^4\text{He}+d$ threshold co-

incide since the two-body system has zero energy). This is clearly a sign of the absence of the symmetric component in the spatial wave function. From the previous discussion we notice the interesting result that, at the unitary limit, there is a mass gap for $A = 5, 6$. This gap continues to exist only for the case $A = 5$ at the physical point.

In fact, following the behavior of the $A = 6$ states from Fig. 3 we observe that, as the two-body system acquires energy, there is a point around $r_0/a_1 \approx 0.07$ in which ${}^6\text{Li}$ emerges from the ${}^4\text{He}+d$ threshold and, at $r_0/a_1 \approx 0.2$, ${}^6\text{He}$ emerges from the ${}^4\text{He}$ threshold. The difference in energy between the two states at this last point is of 2.64 MeV, of the order of the experimental mass difference; it becomes of the order of 5.14 MeV at the physical point. We can conclude that this is a subtle effect of the finite-range character of the force, as we are going to discuss in the next sections.

Finally, we investigate the universal character of the fermionic $A = 6$ states using Eq. (7). A linear behavior of the function $y(\xi)$ indicates a behavior controlled by the scattering lengths and the three-body parameter. In Fig. 4 we plot the value of $y(\xi)$, calculated using the $A = 6$ energies as a function of $\kappa_A^0 a_B$; the latter has been chosen because, at the unitary point, is the energy representing the threshold. We find a dominant linear relation close to the thresholds where the structure of the state is dominated by the ${}^4\text{He}$. For ${}^6\text{Li}$ deviations from the universal behaviour appears close to the physical point whereas the ${}^6\text{He}$ energies follow nicely the linear behavior showing a strongly universal character.

III. THE PHYSICAL POINT

From the calculations of Table I we clearly see that the two-body potential Eq. (1) is too simple to describe the spectrum of light nuclei. On the other hand it captures some important aspects as the one-level three-nucleon spectrum, the E_4/E_3 ratio and the $A = 5$ mass gap. As discussed in the introduction, the two-body Gaussian potential has to be supplemented with a three-body potential devised to reproduce the ${}^3\text{H}$ energy. This corresponds, in Efimov physics, to fix the three-body parameter or, following EFT concepts, the promotion to the LO of the three-body interaction in order to take into account the unnatural large values of the scattering lengths. Here we use an hyper-central three-body potential of the following form

$$W(\rho) = W_0 e^{-(r_{12}^2 + r_{13}^2 + r_{23}^2)/R_3^2}, \quad (8)$$

where r_{ij} is the relative distance between particle i and j . In this potential there are two-independent parameters, the strength of the potential W_0 and its range R_3 . In order to reproduce the ${}^3\text{H}$ binding energy, $E_{3\text{H}} = -8.482$ MeV, an infinite number of pairs (W_0, R_3) can be chosen. However a very small number of such pairs (in fact only two [21]) reproduce other physical inputs

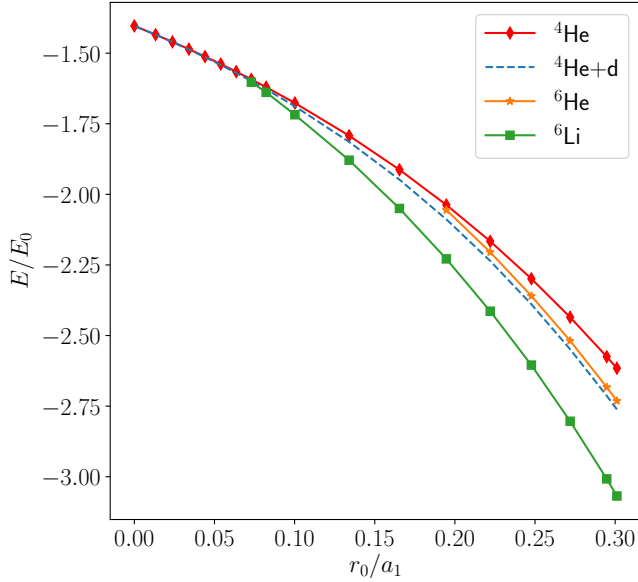


FIG. 3. Efimov plot in the nuclear cut for $A = 6$ particles. The scattering length is in units of $r_0 = 1.65$ fm and the energies in units of $E_0 = \hbar^2/mr_0^2 = 15.232$ MeV. We distinguish between the six-body state that has the quantum numbers of ${}^6\text{He}$ and the one with the quantum numbers of ${}^6\text{Li}$. We also report the energy of the $A = 4$, which has the quantum number of ${}^4\text{He}$, and represents the threshold for the ${}^6\text{He}$, and the energy of ${}^4\text{He}+d$ which represents the threshold for ${}^6\text{Li}$. In the present calculations the Coulomb interaction has not been taken into account.

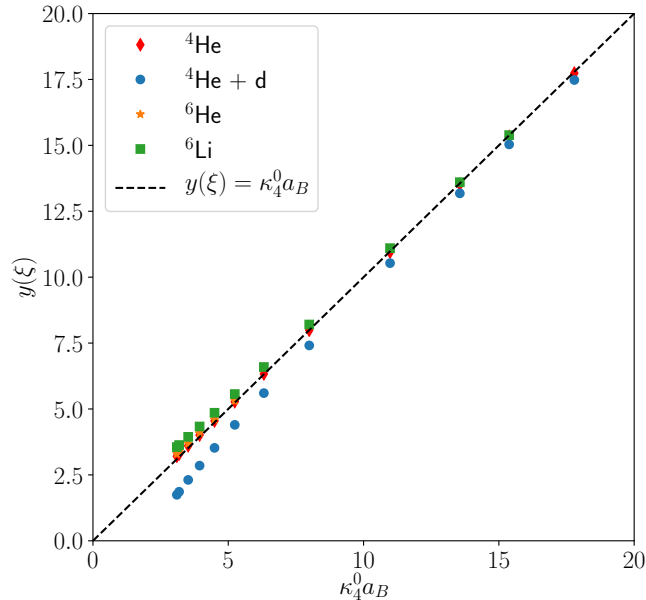


FIG. 4. Efimov plot in the nuclear cut for $A = 6$ particles, the same as in Fig. 3, in the form of $y(\xi)$ as a function of $\kappa_4^0 a_B$. With respect to the $A = 3, 4$ cases, we observe a bigger deviation from the universal prediction of Efimov physics.

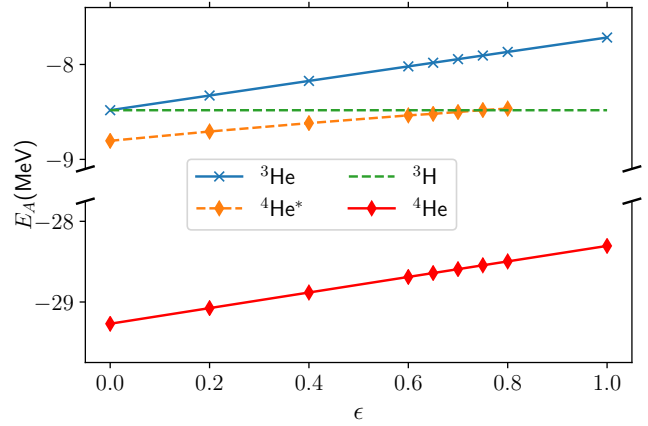


FIG. 5. Evolution of the energies for $A = 3, 4$ as a function of a smooth switching-on of the Coulomb interaction via a multiplicative parameter ϵ . The three-body parameters have been fixed to $W_0 = 7.6044$ MeV and $R_3 = 3.035$ fm. The full Coulomb interaction corresponds to $\epsilon = 1$. The four-body excited state disappears for a critical value $\epsilon^* = 0.754$, while the energies of ${}^3\text{He}$ and ${}^4\text{He}$ goes to the experimental values better than 0.1%.

like the energy of the four-body system or the neutron-deuteron scattering length a_{nd} .

In Table III we show selected parameters of the three-body used to reproduce the energy of ${}^3\text{H}$. In the left part of the table we report calculations without Coulomb interaction; we observe the repulsive nature of the three-body force. Without Coulomb interaction ${}^3\text{He}$ is degenerate with ${}^3\text{H}$ and the four body state has an energy E_4 lower than the one of ${}^4\text{He}$. Moreover, the four-body system shows an unphysical excited state E_4^* ; this is the universal Efimov aspect of nuclear physics: for each three-body state there are two attached four-body states. In the right part of Table III we show calculations where the Coulomb interaction has been taken into account. We observe that there are values of R_3 that allow to reproduce ${}^3\text{He}$, and for these values, the description of ${}^4\text{He}$ is close to the experimental values.

The presence of Coulomb interaction makes the four-body excited state disappear. From the table we select the best value of the three-body force, $W_0 = 7.6044$ MeV and $R_3 = 3.035$ fm, to follow the evolution of the ${}^3\text{He}$ and ${}^4\text{He}$ binding energies as a function of a smooth switching-on of the Coulomb interaction by means of a parameter ϵ . In Table IV we report our calculation as a function of ϵ and the same data are graphically represented in Fig. 5. For $\epsilon = 0$, that means no Coulomb interaction, there is only one three-body bound state and the universal two-attached four-body states. As the value of the Coulomb interaction grows to its full value, $\epsilon = 1$, the degeneracy between the ${}^3\text{H}$ and ${}^3\text{He}$ is removed and also the value of the ground- and excited-state energy of ${}^4\text{He}$ start to change; for $\epsilon \approx 0.75$ the ${}^4\text{He}$ excited state goes behind

TABLE III. Calculation for $A = 3, 4$ at the physical point, $V_{10} = -60.575$ MeV, $V_{01} = -37.9$ MeV, and $E_2 = -2.2255$ MeV, for selected three-body force parameters. In the left part calculations without the Coulomb interaction are reported for ${}^3\text{H}$, E_4 , and E_4^* . In the right part of the table the Coulomb interaction has been included to calculate ${}^3\text{He}$, ${}^4\text{He}$, and the excited state ${}^4\text{He}^*$. The latter disappear as bound state when the three-body force and the Coulomb interaction are consider together. The experimental values are reported in the last row.

$W_0(\text{MeV})$	$R_3(\text{fm})$	${}^3\text{H}(\text{MeV})$	$E_4(\text{MeV})$	$E_4^*(\text{MeV})$	${}^3\text{He}(\text{MeV})$	${}^4\text{He}(\text{MeV})$	${}^4\text{He}^*(\text{MeV})$
0	-	-10.2455	-39.843	-11.193	-9.426	-38.789	-10.655
11.922	2.5	-8.48	-28.670	-8.75	-7.722	-27.754	-
9.072	2.8	-8.48	-29.014	-8.79	-7.718	-28.060	-
7.8	3.0	-8.48	-29.223	-8.80	-7.715	-28.258	-
7.638	3.03	-8.48	-29.255	-8.80	-7.714	-28.290	-
7.612	3.035	-8.48	-29.260	-8.80	-7.714	-28.295	-
7.6044	3.035	-8.482	-29.269	-8.80	-7.716	-28.305	-
Experimental Values		-8.482			-7.718	-28.296	

TABLE IV. Calculation for $A = 3, 4$ for the case $W_0 = 7.6044$ MeV and $R_3 = 3.035$ fm with a slow switch on of Coulomb interaction controlled by the parameter ϵ . The threshold of ${}^3\text{H}+p$ is $E_{3\text{H}} = -8.482$ MeV, which implies that the four-body excited state ${}^4\text{He}^*$ is no more bounded for $\epsilon \approx 0.75$.

ϵ	${}^3\text{He}(\text{MeV})$	${}^4\text{He}(\text{MeV})$	${}^4\text{He}^*(\text{MeV})$
0	-8.482	-29.269	-8.804
0.2	-8.327	-29.076	-8.706
0.4	-8.173	-28.882	-8.618
0.6	-8.020	-28.689	-8.536
0.65	-7.982	-28.641	-8.520
0.7	-7.944	-28.593	-8.501
0.75	-7.906	-28.545	-
0.8	-7.868	-28.497	-
1	-7.716	-28.305	-

the ${}^3\text{H}+p$ threshold; a polynomial fit gives the value of threshold at $\epsilon^* = 0.754$. One can probably expect that the fate of this excited state is to become the known 0^+ resonance of ${}^4\text{He}$; in order to see this, one should follow the state as it enters the continuum and mixes with it. Some preliminary studies do not support this picture, but there are some indication that the state becomes a virtual state. Just as an exercise, we can make a simple extrapolation; the result of such an exercise is reported in Fig. 6, where the extrapolated energy is at -8.40 MeV, quite far from the experimental energy of the resonance (-8.0860 MeV).

To summarise this section, a simple Gaussian-potential acting mainly on $L = 0$ supplemented with a three-body force and the Coulomb interaction describes quite accurately the spectrum of light nuclei up to four nucleons. The emerging DSI, controlled by the values of the scattering lengths and the three-nucleon binding energy, strongly constrains the spectrum inside the universal window. Here we would like to see to which extent the energies of ${}^6\text{He}$ and ${}^6\text{Li}$ are correlated by those param-

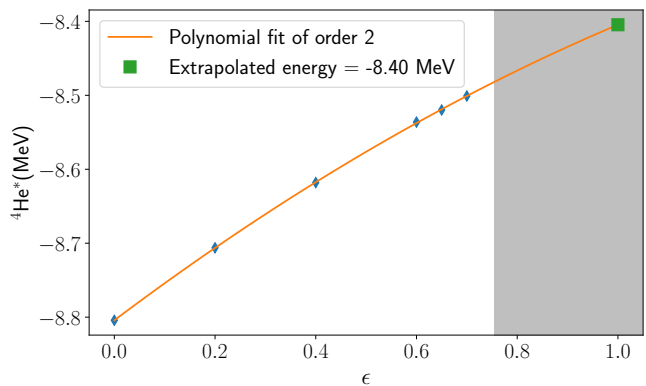


FIG. 6. Energy of the excited four body state ${}^4\text{He}^*$ as a function of the switching-on of the Coulomb interaction. The grey zone indicates the continuum, which the state enters at $\epsilon^* = 0.754$. We extrapolate the state up to full Coulomb $\epsilon = 1$, but this does not mean that the extrapolated energy corresponds to a resonance because we are not taking into account the mixing with the continuum. The experimental position of 0^+ resonance of ${}^4\text{He}$ is -8.086 MeV.

eters. Though the thresholds are well determined, our observation is that the $L = 0$ force, even without considering the Coulomb interaction, is not able to bound the six-fermion system.

IV. RÔLE OF P -WAVES

From the previous discussion we have seen that the simple version of the nuclear interaction dictated by the Efimov physics is not enough to describe the six-body sector of the light nuclei spectrum. In this section we investigate the possible rôle of the two terms of the potential Eq. (1), V_{00} , and V_{11} , that in the previous sections have been set to zero. These terms contribute to the description of the P -waves through the antisymmet-

ric condition $(-1)^{(L+S+T)} = -1$. At the two-body level the low energy P -wave phase-shifts can be described by an effective range expansion which, for single channels, is of the form

$$S_k = k^3 \cot^{2S+1} P_J = \frac{-1}{2^{2S+1} a_J} + \frac{1}{2} {}^{2S+1} r_J k^2, \quad (9)$$

where ${}^{2S+1} P_J$ is the P -wave phase-shift in spin channel S coupled to total angular momentum J , ${}^{2S+1} a_J$ is the scattering volume and ${}^{2S+1} r_J$ is the P -wave effective range. In Fig.7 the effective range function S_k is shown for the uncoupled phases calculated using the AV14 nucleon-nucleon interaction [40] (circles) together with a fit for those results (solid lines). The linear behavior is well verified in this energy region and allows to extract the scattering parameters as given in Table V.

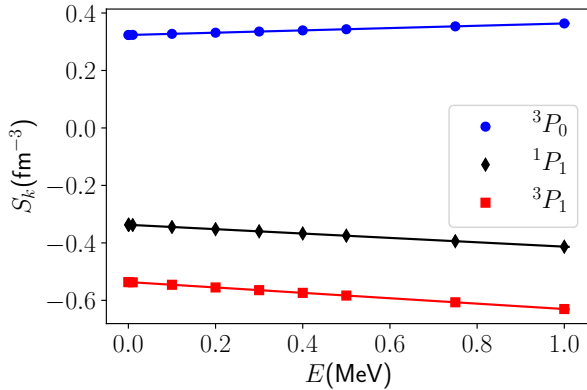


FIG. 7. P -wave phase shifts calculated using the AV14 nucleon-nucleon interaction. The points are the effective calculations, while the solid lines are fits to that data allowing to extract the scattering parameters, see Table V.

TABLE V. Scattering parameters of the effective range expansion Eq (9) for the P -wave phase shift.

${}^{2S+1} a_J$ [fm $^{-3}$]	${}^{2S+1} r_J$ [fm $^{-1}$]
${}^1 a_1$ 1.437	${}^1 r_1$ -6.308
${}^3 a_1$ 1.231	${}^3 r_1$ -7.786
${}^3 a_0$ -1.457	${}^3 r_0$ 3.328

From the above analysis we can observe that the interaction in channel $S, T = 0, 0$ is repulsive whereas the interaction in channel $S, T = 1, 1$ is slightly attractive in $J = 0$ wave. In the first case, we reproduce the scattering data with the interaction

$$V_{00} = +1.625 \text{ MeV} \quad r_{00} = 4.03 \text{ fm}; \quad (10)$$

with this choice, even ${}^1 P_1$ phases are well described. The ${}^3 P_0$ phases are well described with the interaction

$$V_{11} = -3.857 \text{ MeV} \quad r_{11} = 3.35 \text{ fm}. \quad (11)$$

However the interaction defined in Eq.(1) cannot distinguish between the different two-body J -states. Accordingly, for the $S, T = 1, 1$ channel we use a Gaussian interaction with range $r_{11} = 3.35$ and we allow variations of the strength around the value -3.857 MeV. We make one step further and we optimize the interactions in V_{10} and V_{01} to describe the $L = 0$ singlet and triplet scattering lengths and corresponding effective ranges. The choice for the potentials is the following

$$\begin{aligned} V_{01} &= -30.545885 \text{ MeV} & r_{01} &= 1.8310 \text{ fm} \\ V_{10} &= -66.5824776 \text{ MeV} & r_{10} &= 1.5579 \text{ fm}. \end{aligned} \quad (12)$$

The potential of Eq.(1) is now defined in the four S, T components and, as in the previous calculations, we introduce a three-body force to fix the value of the ${}^3\text{H}$. We use two different range R_3 to explore how the six bodies depend on it.

In Table VI we report our calculations for different choices of the strength V_{11} and the corresponding three-body strength W_0 . In all cases the binding energies of ${}^3\text{He}$ and ${}^4\text{He}$ are well described considering that the only charge symmetry breaking component of the force taken into account is the Coulomb interaction. It is interesting to notice that the inclusion of the very weak attraction in channel $S, T = 1, 1$ is enough to bind ${}^6\text{He}$ and ${}^6\text{Li}$ though their bindings are a little bit overpredicted (see first row of the table). By decreasing the V_{11} strength it is possible to describe better the ${}^6\text{He}$ binding energy, as for example using the strength -2.5 MeV, but ${}^6\text{Li}$ remains overbind by around 1 MeV. This is a consequence of the lack of flexibility of the force defined in Eq.(1) to distinguish between the different states in the two-body P -channels. This can be achieved by a spin-orbit term which can remove the degeneracy between the three ${}^3 P_J$ phase shifts. In fact the present interaction predicts a difference ${}^6\text{Li} - {}^6\text{He}$ mass more or less constant, 1 MeV greater than the experimental value. In Fig. 8 the results for the six-body sector are represented; on top of each data we write the range of the three-body force we used. We observe a linear dependence of the energies with respect the strength of V_{11} potential, while the different three-body ranges just shift the linear dependence.

V. CONCLUSIONS

The fact that the two s -wave scattering lengths, a_0 and a_1 , are large with respect the natural size of the NN interaction, locates nuclear physics inside the universal window. In this context is of interest analyze the spectrum of $1/2$ spin-isospin fermions controlled by these two parameters. This very simplified picture has been studied in the first part of the present work up to six fermion using a Gaussian potential model with variable strength. Assigning values to the Gaussian strengths in the spin-isospin channels $S, T = 0, 1$ and $1, 0$ the two scattering lengths, a_0 and a_1 , were allowed to vary from infinite to

TABLE VI. For each choice of the V_{11} potential the three-body force has been tuned to reproduce the energy of the ${}^3\text{H}$. The range of the potential has been fixed to $r_{11} = 3.35$ fm.

V_{11} (MeV)	W_0 (MeV)	R_3 (fm)	${}^3\text{He}$ (MeV)	${}^4\text{He}$ (MeV)	${}^6\text{He}$ (MeV)	${}^6\text{Li}$ (MeV)
-3.857	7.8375	1.4	-7.746	-28.32	-30.93	-34.86
-3.0	7.8104	1.4	-7.746	-28.34	-29.90	-33.67
-3.0	13.461	1.2	-7.749	-28.20	-30.43	-34.35
-2.5	7.7940	1.4	-7.745	-28.35	-29.25	-33.07
-2.5	13.433	1.2	-7.749	-28.21	-29.81	-33.63
-2.0	13.405	1.2	-7.749	-28.22	-29.16	-32.93
-1.78	13.392	1.2	-7.749	-28.23	-28.87	-32.64
Experimental Values			-7.718	-28.296	-29.268	-31.9938

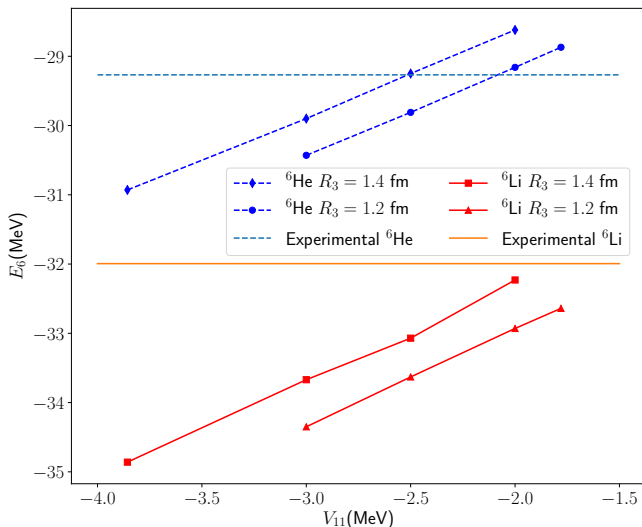


FIG. 8. Energy of ${}^6\text{He}$ and ${}^6\text{Li}$ as a function of the potential strength V_{11} . The number on top of each point represent the value of the three-body range R_3 that has been used. For the sake of comparison, we also draw the experimental values.

their physical values following a path, called nuclear cut, in which the ratio $a_0/a_1 = -4.3066$ were kept constant. Considering only two-body Gaussians and disregarding the Coulomb interaction, the main results of this analysis are shown in Fig. 1 and Fig. 3 where the main characteristic of the six fermion spectrum can be seen. At unitary the $A = 5, 6$ nuclei are not bound from the $A = 4$ threshold. As the system moved from unitary through the physical point, the tower of infinite three-body states disappear with only one state surviving. At the same time the six-body system becomes bound, first the state having the ${}^6\text{Li}$ quantum numbers and then the state having the ${}^6\text{He}$ quantum numbers. Moreover all along the path the excited state of ${}^4\text{He}$ is bound with respect to the three-nucleon threshold. Though the values of the energies are not well reproduced using a two-body Gaussian interaction, the spectrum at the physical point is formed by one two-nucleon state, one three-nucleon state, two

four-nucleon states and two six-nucleon states.

Two ingredients are missing in this analysis. The first one is trivial and consists in the inclusion of the Coulomb interaction. The second ingredient is dictated by EFT concepts and consists in the consideration of a three-body force. Accordingly, in the second part of the study we concentrate in the physical point considering those terms in the interaction. The main results are given in Table III where selected parametrization of the three-body force are shown in order to describe the triton binding energy. It should be noticed that considering the Coulomb interaction without including the three-body force or, vice versa, considering the three-body force without including the Coulomb interaction, produces a four-nucleon spectrum with two bound states. The three- and four-nucleon spectra go to the correct place after including both interactions. A detailed study of how the ${}^4\text{He}^*$ excited state crosses the threshold to the ${}^3\text{H}-p$ continuum is given in Fig 6. Preliminary studies indicate that, with the simply interaction used here, the ${}^4\text{He}^*$ excited state becomes a virtual state. Furthermore, when both, the Coulomb interaction and the three-body force, are taken into account the two six-fermion states become unbound.

The repulsive character of the three-body force, needed to fix the triton binding energy, produces a delicate cancellation between the different energy terms promoting both ${}^6\text{Li}$ and ${}^6\text{He}$ above the respective thresholds. In order to see how these two nuclei emerge from their thresholds, in the final part of this study, we extend the Gaussian potential model to include interactions in the spin-isospin channels $S, T = 0, 0$ and $1, 1$. The strengths and ranges of these terms have been fixed to reproduce the NN P -wave effective range expansion, as given for example by the AV14 interaction. Our observation was that a very weak attractive force in the $S, T = 1, 1$ channel is sufficient to bind ${}^6\text{Li}$ and ${}^6\text{He}$, however with their mass difference overpredicted by 1 MeV.

The present analysis supports the picture of an universal window in which the light nuclear systems are located. To this respect the three control parameters, the two-scattering lengths and the triton binding energy, fix the spectrum of $A \leq 4$ nuclei, explain the number of levels, the $A = 5$ mass gap and locate the $A = 6$ thresholds.

The very weak binding of the $A = 6$ nuclei below the ${}^4\text{He}$ and ${}^4\text{He}+d$ thresholds are due to a weakly attractive P -wave interaction. A more quantitative description of these weakly bound states necessitates the considera-

tion of a more complex set of operators in the interactions as a spin-orbit force. For a similar analysis in the context of chiral perturbation theory we refer to the recent work [41].

-
- [1] Eric Braaten and H.-W. Hammer, “Universality in few-body systems with large scattering length,” *Physics Reports* **428**, 259–390 (2006).
- [2] V Efimov, “Energy levels arising from resonant two-body forces in a three-body system,” *Phys. Lett. B* **33**, 563–564 (1970).
- [3] V Efimov, “Weak Bound States of Three Resonantly Interacting Particles,” *Sov. J. Nucl. Phys.* **12**, 589 (1971), [*Yad. Fiz.* **12**, 1080–1090 (1970)].
- [4] Cheng Chin, Grimm, Rudolf, Paul Julienne, and Eite Tiesinga, “Feshbach resonances in ultracold gases,” *Rev. Mod. Phys.* **82**, 1225–1286 (2010).
- [5] Fei Luo, George C. McBane, Geunsik Kim, Clayton F. Giese, and W. Ronald Gentry, “The weakest bond: Experimental observation of helium dimer,” *J. Chem. Phys.* **98**, 3564 (1993).
- [6] E. Wigner, “On the Mass Defect of Helium,” *Phys. Rev.* **43**, 252–257 (1933).
- [7] Enrico Fermi, “Sul moto dei neutroni nelle sostanze idrogenate,” *Ricerca sci.* **7**, 13–52 (1936).
- [8] Kerson Huang and C. N. Yang, “Quantum-Mechanical Many-Body Problem with Hard-Sphere Interaction,” *Phys. Rev.* **105**, 767–775 (1957).
- [9] Eric Braaten and H.-W. Hammer, “An Infrared Renormalization Group Limit Cycle in QCD,” *Phys. Rev. Lett.* **91**, 102002 (2003).
- [10] E. Epelbaum, H.-W. Hammer, U.-G. Meißner, and A. Nogga, “More on the infrared renormalization group limit cycle in QCD,” *Eur. Phys. J. C* **48**, 169–178 (2006).
- [11] S.R. Beane, P.F. Bedaque, M.J. Savage, and U. van Kolck, “Towards a perturbative theory of nuclear forces,” *Nucl. Phys. A* **700**, 377–402 (2002).
- [12] U. van Kolck, “Effective field theory of short-range forces,” *Nuclear Physics A* **645**, 273–302 (1999).
- [13] P. Bedaque, H.-W. Hammer, and U. van Kolck, “Renormalization of the Three-Body System with Short-Range Interactions,” *Phys. Rev. Lett.* **82**, 463–467 (1999).
- [14] P. F. Bedaque, H. W. Hammer, and U. van Kolck, “The three-boson system with short-range interactions,” *Nucl. Phys. A* **646**, 444 – 466 (1999).
- [15] Harald W. Grißhammer, “Naïve dimensional analysis for three-body forces without pions,” *Nucl. Phys. A* **760**, 110–138 (2005).
- [16] A. Kievsky, M. Viviani, M. Gattobigio, and L. Girlanda, “Implications of Efimov physics for the description of three and four nucleons in chiral effective field theory,” *Phys. Rev. C* **95** (2017), 10.1103/PhysRevC.95.024001.
- [17] M. Gattobigio, A. Kievsky, and M. Viviani, “Spectra of helium clusters with up to six atoms using soft-core potentials,” *Phys. Rev. A* **84**, 052503 (2011).
- [18] A. Kievsky, N. K. Timofeyuk, and M. Gattobigio, “ $\$N\$$ -boson spectrum from a discrete scale invariance,” *Phys. Rev. A* **90**, 032504 (2014).
- [19] A. Kievsky, A. Polls, B. Juliá-Díaz, and N. K. Timofeyuk, “Saturation properties of helium drops from a leading-order description,” *Phys. Rev. A* **96** (2017), 10.1103/PhysRevA.96.040501.
- [20] A Bulgac and V Efimov, “Spin dependence of the level spectrum of three resonantly interacting particles,” *Sov. J. Nucl. Phys.* **22**, 153 (1976).
- [21] A. Kievsky and M. Gattobigio, “Efimov Physics with $1/2$ Spin-Isospin Fermions,” *Few-Body Syst* **57**, 217–227 (2016).
- [22] A. Kievsky and M. Gattobigio, “ $1/2$ spin-isospin fermions close to the unitary limit,” *Journal of Physics: Conference Series* **981**, 012021 (2018).
- [23] Sebastian König, Harald W. Grißhammer, H.-W. Hammer, and U. van Kolck, “Nuclear Physics Around the Unitarity Limit,” *Phys. Rev. Lett.* **118** (2017), 10.1103/PhysRevLett.118.202501.
- [24] U van Kolck, “Nuclear physics from an expansion around the unitarity limit,” *Journal of Physics: Conference Series* **966**, 012014 (2018).
- [25] H.-W. Hammer, “Nuclei and the Unitary Limit,” *Few-Body Systems* **59** (2018), 10.1007/s00601-018-1386-7.
- [26] S. R. Beane, P. F. Bedaque, L. Childress, A. Kryjevski, J. McGuire, and U. van Kolck, “Singular potentials and limit cycles,” *Phys. Rev. A* **64**, 042103 (2001).
- [27] R. Álvarez-Rodríguez, A. Deltuva, M. Gattobigio, and A. Kievsky, “Matching universal behavior with potential models,” *Phys. Rev. A* **93**, 062701 (2016).
- [28] A. Kievsky, L. E. Marcucci, S. Rosati, and M. Viviani, “High-Precision Calculation of the Triton Ground State Within the Hyperspherical-Harmonics Method,” *Few-Body Syst* **22**, 1–10 (1997).
- [29] M. Gattobigio, A. Kievsky, M. Viviani, and P. Barletta, “Harmonic hyperspherical basis for identical particles without permutational symmetry,” *Phys. Rev. A* **79**, 032513 (2009).
- [30] M. Gattobigio, A. Kievsky, M. Viviani, and P. Barletta, “Non-symmetrized Basis Function for Identical Particles,” *Few-Body Syst.* **45**, 127–131 (2009).
- [31] M. Gattobigio, A. Kievsky, and M. Viviani, “Nonsymmetrized hyperspherical harmonic basis for an A-body system,” *Phys. Rev. C* **83**, 024001 (2011).
- [32] K. Varga and Y. Suzuki, “Precise solution of few-body problems with the stochastic variational method on a correlated Gaussian basis,” *Phys. Rev. C* **52**, 2885–2905 (1995).
- [33] A. Deltuva, “Properties of Universal Bosonic Tetramers,” *Few-Body Syst* **54**, 569–577 (2013).
- [34] M. Gattobigio, M. Göbel, H.-W. Hammer, and A. Kievsky, “More on the universal equation for Efimov states,” arXiv (2019), arXiv:1903.05493 [cond-mat, physics:nucl-th].
- [35] M. Gattobigio and A. Kievsky, “Universality and scaling in the $\$N\$$ -body sector of Efimov physics,” *Phys. Rev. A* **90**, 012502 (2014).
- [36] M Gattobigio and A Kievsky, “Some aspects of universality in Efimov physics,” *Journal of Physics: Conference*

- Series **527**, 012002 (2014).
- [37] Chen Ji, Eric Braaten, Daniel R. Phillips, and Lucas Platter, “Universal relations for range corrections to Efimov features,” *Phys. Rev. A* **92** (2015), 10.1103/PhysRevA.92.030702.
- [38] B. S. Pudliner, V. R. Pandharipande, J. Carlson, and R. B. Wiringa, “Quantum Monte Carlo Calculations of $A \leq 6$ Nuclei,” *Phys. Rev. Lett.* **74**, 4396–4399 (1995).
- [39] M. Gattobigio, A. Kievsky, and M. Viviani, “Energy spectra of small bosonic clusters having a large two-body scattering length,” *Phys. Rev. A* **86**, 042513 (2012).
- [40] R. B. Wiringa, R. A. Smith, and T. L. Ainsworth, “Nucleon-nucleon potentials with and without Δ (1232) degrees of freedom,” *Phys. Rev. C* **29**, 1207–1221 (1984).
- [41] Bing-Nan Lu, Ning Li, Serdar Elhatisari, Dean Lee, Evgeny Epelbaum, and Ulf-G. Meißner, “Essential elements for nuclear binding,” arXiv (2018), arXiv:1812.10928 [hep-lat, physics:nucl-th].